

# A method to calculate basin bifurcation sets for a two-dimensional noninvertible map

Hiroyuki Kitajima, Hiroshi Kawakami† and Christian Mira‡

*Dept. of Reliability-based Information Systems Engineering, Kagawa University, Takamatsu, 760-8526 Japan*  
kitaji@eng.kagawa-u.ac.jp

†*Dept. of Electrical and Electronic Engineering, The University of Tokushima, Tokushima, 770-8506 Japan*  
kawakami@ee.tokushima-u.ac.jp

‡*GENSLA-LESIA, INSA, Complexe Scientifique de Rangueil, 31077 Toulouse, France*  
mira@dge.insa-tlse.fr

**Abstract**— In this paper we propose a numerical method to calculate basin bifurcation sets in a parameter space. It is known that the basin bifurcations always result from the contact of a basin boundary with the critical curve segment. A numerical example for a two-dimensional quadratic noninvertible map is illustrated and new results of basin bifurcations are shown.

## I. Introduction

It is worth noting that many systems in engineering, particularly in control theory and electronics, lead to models expressed by noninvertible maps. This is particularly the case in some control systems using sampled data, switching elements or pulse modulation, and also in some adaptive controls [1, 2]. Moreover, modeling in economics [3] and biology [4] often gives rise to noninvertible maps.

For the analysis of two-dimensional noninvertible maps (e.g. basin bifurcation, definition of absorbing and chaotic areas, homoclinic and heteroclinic points, and their bifurcations, formation of self intersection of the unstable manifold of a saddle fixed point and so on), it is known that a critical curve (abbrev.  $LC$  for “Ligne Critique” in French) and a curve of merging preimages ( $LC_{-1}$ : the first rank preimages of  $LC$ ) play an essential role. The critical curve is the two-dimensional generalization of the notion of critical point of one-dimensional endomorphism. When the map is continuous and continuously differentiable (of class  $C^1$ ), then the curve of merging preimages ( $LC_{-1}$ ) is included in the set defined by  $J = 0$ , where  $J$  denotes the Jacobian determinant of the map.

To our knowledge, for studying two-dimensional endomorphisms, the notation of critical curve was first introduced in 1964 in relation to its role in the determination of basin boundaries [5]. Since 1969, several papers have developed the role of critical curves in the basin bifurcations called “simply connected basin  $\Leftrightarrow$  disconnected basin” and “simply connected basin  $\Leftrightarrow$  multiply connected basin” [6]. Even now these are hot topics [7], because the basin bifurcations may corre-

spond to global bifurcations and may have interesting structure fundamentally different from those produced by an invertible map. These basic basin bifurcations always result from the contact of a basin boundary with the critical curve segment and are generated by the same basic mechanisms. Now, we know the mechanisms of the basic basin bifurcations, however in general there are no systematic methods to obtain the bifurcation value of the system parameter. If we know the set of bifurcation values in the parameter space, we can design a system with the optimal operating condition. Therefore we need an algorithm to obtain these bifurcation parameter values for setting the system parameter.

## II. Definition of system

We consider a two-dimensional noninvertible map as a function of a parameter  $\lambda$  defined by

$$T_\lambda : R^2 \rightarrow R^2; (x, y) \mapsto (x', y'). \quad (1)$$

The singular set of  $T_\lambda$  is denoted by  $LC_{-1}$ :  $LC_{-1} = \{X \in R^2 \mid \det DT_\lambda(X) = 0\}$ , where  $DT_\lambda$  is the derivative of  $T_\lambda$  (Jacobian matrix). The set  $T_\lambda^m(LC_{-1})$  is denoted by  $LC_{m-1}$ , in particular when  $m = 1$  it is called critical curve ( $LC$ ).

Here we assume that the critical curve  $LC$  separates  $R^2$  into two open regions  $Z_0$  and  $Z_2$ . A point  $X$  belonging to  $Z_2$  has two distinct preimages and a point  $X$  of  $Z_0$  is without preimages. Therefore the map (1) is called  $(Z_0, Z_2)$  type and has simplest properties of a noninvertible map.

## III. Method

In this section we explain the algorithm for obtaining the parameter of the tangent point of critical curve and basin boundary (see Fig. 1(b)). This parameter is called basin bifurcation value, because the basin undergo a qualitative change. For obtaining the initial conditions of Fig. 1(b), we also consider the case of Fig. 1(a).

Now, the problem is “*how to calculate basin boundary which is tangent to LC ?*” Generally speaking, the

basin boundary is given by global stable invariant set  $W_S(D^n)$ , where  $D^n$  is saddle type  $n$ -periodic points satisfying

$$T_\lambda^n(D^n) = D^n \quad (2)$$

on the basin boundary. Let  $U$  be a neighborhood of  $D^n$ . Then using the local stable invariant set  $W_S^L(D^n)$ ,  $W_S(D^n)$  which is tangent to  $LC$  is given by  $(W_S^L(D^n))_{-m}$  (rank- $m$  preimages of  $W_S^L(D^n)$ ), where  $m$  is a positive integer [9]. Note that when  $T_\lambda$  is a non-invertible map,  $W_S(D^n)$  may be non-connected and made of infinitely many closed curves.

Moreover, using next property [10]:

**[property 1]** If a curve  $C$  and  $LC$  intersect at a point  $P$ , then  $T_\lambda^l(C)$  and  $LC_l$  meet tangentially at  $T_\lambda^l(P)$ , where  $LC_l = T_\lambda^l(LC)$  and  $l$  is any integer,

we calculate the tangent point of  $W_S^L(D^n)$  and  $LC_m$  instead of  $(W_S^L(D^n))_{-m}$  and  $LC$ , for simplicity (see Fig. 2). The intersecting (or tangent) point  $P$  in Fig. 1 is equivalent to  $Q_0$  in Fig. 2.

### A. Transverse type

We take an  $\epsilon$ -neighborhood  $U(\epsilon, D^n)$  as shown in Fig. 2(a) [11, 12], then there exists a positive integer  $M$  such that

$$Q_0 = T_\lambda^{-M}(Q_M), \quad Q_M \in U(\epsilon, D^n). \quad (3)$$

The map  $T_\lambda$  is noninvertible, however in the region  $Z_2$  it is possible to explicitly compute the inverse map. To calculate preimages of general noninvertible maps, see Ref. [13]. From **property 1**, the point  $Q_0$  also satisfies

$$Q_0 = T_\lambda^m(P). \quad (4)$$

Substituting Eq. (4) into Eq. (3), we obtain

$$T_\lambda^m(P) - T_\lambda^{-M}(Q_M) = 0 \quad (5)$$

Here we use the first order approximation or eigenvector as the linearization of  $W_S^L$  in the  $\epsilon$ -neighborhood. The condition such that the point  $Q_M$  is included in  $W_S^L$  is written as

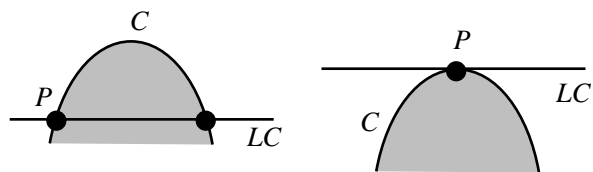
$$W_S^*(Q_M - D^n) = 0 \quad (6)$$

where the row vector  $W_S^*$  is

$$W_S^* = \begin{pmatrix} 1 & 0 \\ 0 & 1 \end{pmatrix} (\mu_\omega I - DT_\lambda), \quad \text{or} \quad (7)$$

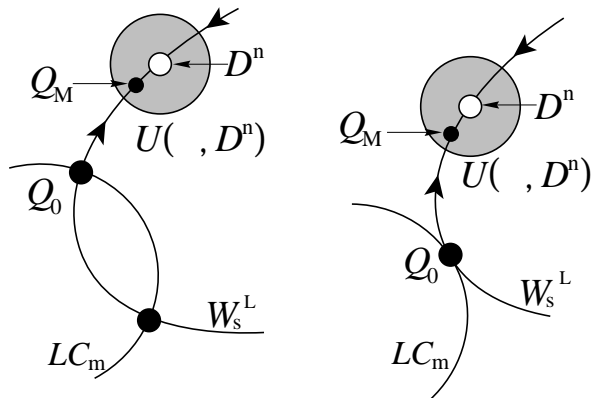
In the equation,  $DT_\lambda$  indicates the derivative of  $T_\lambda$  with respect to the  $n$ -periodic points  $D^n$ , and  $|\mu_\omega| < 1$  denotes the characteristics multiplier.

If  $W_S^L$  intersects the curve  $LC_m$  at the point  $Q_0$ , then Eq. (6) is independent of Eq. (5). Therefore we can determine variables  $(P, Q_M) \in R^3$  for the set of Eq. (5) and (6). (Note that  $P$  is a one-dimensional variable, because  $P$  is on  $LC$ .)



(a) Transverse type. (b) Non-transverse type.

Figure 1: Two types of intersecting points ( $P$ ) of basin boundary ( $C$ ) and critical curve ( $LC$ ).



(a) Transverse type. (b) Non-transverse type.

Figure 2: Equivalent situation to Fig. 1.

### B. Non-transverse type

Let

$$\phi: R \rightarrow R^2; \quad s \mapsto \phi(s) \quad (8)$$

be a representation of  $W_S^L$  in  $U(\epsilon, D^n)$ , where  $\phi(0) = D^n$  and  $\phi(s_\omega) = Q_M$ .

We now consider the derivative of  $\phi$  with respect to  $s$ , that is,

$$\frac{d\phi}{ds}(s) = V(\phi(s)) \quad (9)$$

then we have a tangent vector of  $W_S^L$  at the point  $Q_0$

$$\begin{aligned} \left. \frac{d(T_\lambda^{-M} \circ \phi)}{ds} \right|_{s=s_\omega} &= DT_\lambda^{-M}(\phi(s_\omega)) \frac{d\phi}{ds}(s_\omega) \\ &= DT_\lambda^{-M}(Q_M) V_{S_0} \end{aligned} \quad (10)$$

where  $V(\phi(s_\omega)) = V_{S_0}$ , for simplicity. Hence we have a condition for coincidence of the directions of  $W_S^L$  and  $LC_m$ :

$$\left| DT_\lambda^{-M}(Q_M) V_{S_0} : DT^m(P) \begin{pmatrix} \alpha \\ \beta \end{pmatrix} \right| = 0 \quad (11)$$

where  $V_{S_0}$  is the eigenvector (linearized  $W_S^L$  in  $\epsilon$ -neighborhood) and  $(\alpha \ \beta)^T$  is the tangent vector of  $LC$  at the point  $P$ . Hence the problem is reduced to determine variables  $(D^n, P, Q_M, \lambda) \in R^6$  for the set of Eqs. (2), (5), (6) and (11).

## IV. Numerical Example

We illustrate numerical results for the following map:

$$x_{n+1} = ax_n + y_n, \quad y_{n+1} = x_n^2 + b. \quad (12)$$

The critical curve  $LC$  is defined by  $y = b$ . We calculate the tangent point of  $LC$  and a basin boundary formed by a stable invariant set of saddle type periodic points. Therefore in advance we must know the location and period of the saddle type periodic points on the boundary, using, e.g., a bifurcation diagram for periodic points.

We obtain a bifurcation diagram (see Fig. 3) of 5-periodic points using Kawakami's method [14]. In this figure,  $G$ ,  $I$  and  $N$  represent tangent (fold), period-doubling (flip) and Neimark-Sacker bifurcation sets of 5-periodic points, respectively. To explain the bifurcation phenomena for 5-periodic points in Fig. 3, we change the parameter  $b$  along the line  $L$ . By the tangent bifurcation set  $G$  (marked by ① in Fig. 3), two 5-periodic points:  ${}_0D^5$  and  ${}_1D^5$  (superscript and subscript of  $D$  indicate period and unstable subspace of periodic points, respectively) appear. The stable 5-periodic points  ${}_0D^5$  exist in the shaded region. In this region we can calculate the basin of the 5-periodic points. On the period-doubling bifurcation set  $I$  of the unstable 5-periodic points  ${}_1D^5$  (②), there appear saddle type 10-periodic points  ${}_1D^{10}$ . Hence we use the 10-periodic points as  $D^n$  mentioned in Sec. 3. On the Neimark-Sacker bifurcation set  $N$  of the stable 5-periodic points (③), the 5-periodic points become unstable and generate quasi-periodic solutions (5 invariant closed curves).

By using the method proposed in Sec. 3, we obtain basin bifurcation sets  $B$  shown in also Fig. 3. Figure 4 shows an enlarged diagram of Fig. 3. Note that we do not calculate all the basin bifurcation sets in this parameter region. The basin bifurcation sets  $B_1$  to  $B_5$  separate the parameter  $(a, b)$  plane into six parts. In each part we calculate basin for 5-periodic points and show them in Fig. 5(a) to (h). In each figure the plane is the set of initial state  $(x_0, y_0)$  and the solution which starts from the outside region of basin goes to infinity. The basin is classified into 5 different colors. At the point marked (a) in Fig. 4, there exists a *simply connected basin* (see Fig. 5(a)). On the curve  $B_1$ , one of the basin boundary touches the critical curve  $LC$ . As a result there appear *holes* in the basin (Fig. 5(b)) and *simply connected basin* becomes *multiply connected basin* (Fig. 5(c)). By crossing the bifurcation curves  $B_2$  and  $B_3$ , basin Fig. 5(c) bifurcates to Fig. 5(d) and (e), respectively. In Fig. 5(e) two different holes  $H^2$  and  $H^3$  appear in hole  $H^1$ . By crossing the bifurcation curves  $B_4$  and  $B_5$  again, basin Fig. 5(f) bifurcates to Fig. 5(g) and (h), respectively.

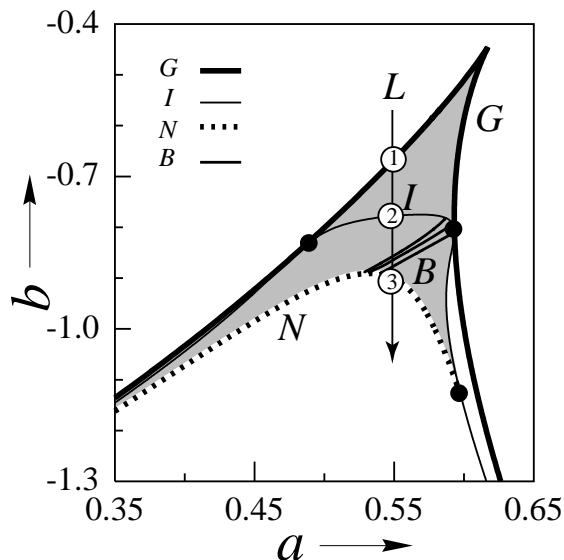


Figure 3: Bifurcation sets of 5-periodic points ( $G$ ,  $I$  and  $N$ ) and basin bifurcation sets ( $B$ ).

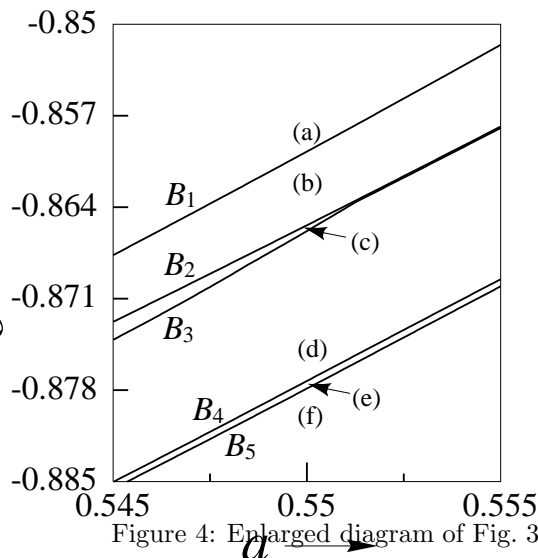


Figure 4: Enlarged diagram of Fig. 3.

We can see the occurrence of successive basin bifurcations.

## V. Conclusions

We proposed the numerical method to calculate basin bifurcation values. At this parameter the critical curve is tangent to a stable invariant set of saddle type periodic points on the basin boundary. We derived some bifurcation conditions and solved them numerically. We only showed the algorithm for “simply connected basin  $\Leftrightarrow$  multiply connected basin”, but our algorithm is applicable to the other basin bifurcations classified in Ref. [8].

As an illustrated example, we showed basin bifurcation diagrams for a two-dimensional quadratic non-invertible map. In the bifurcation diagram, we found

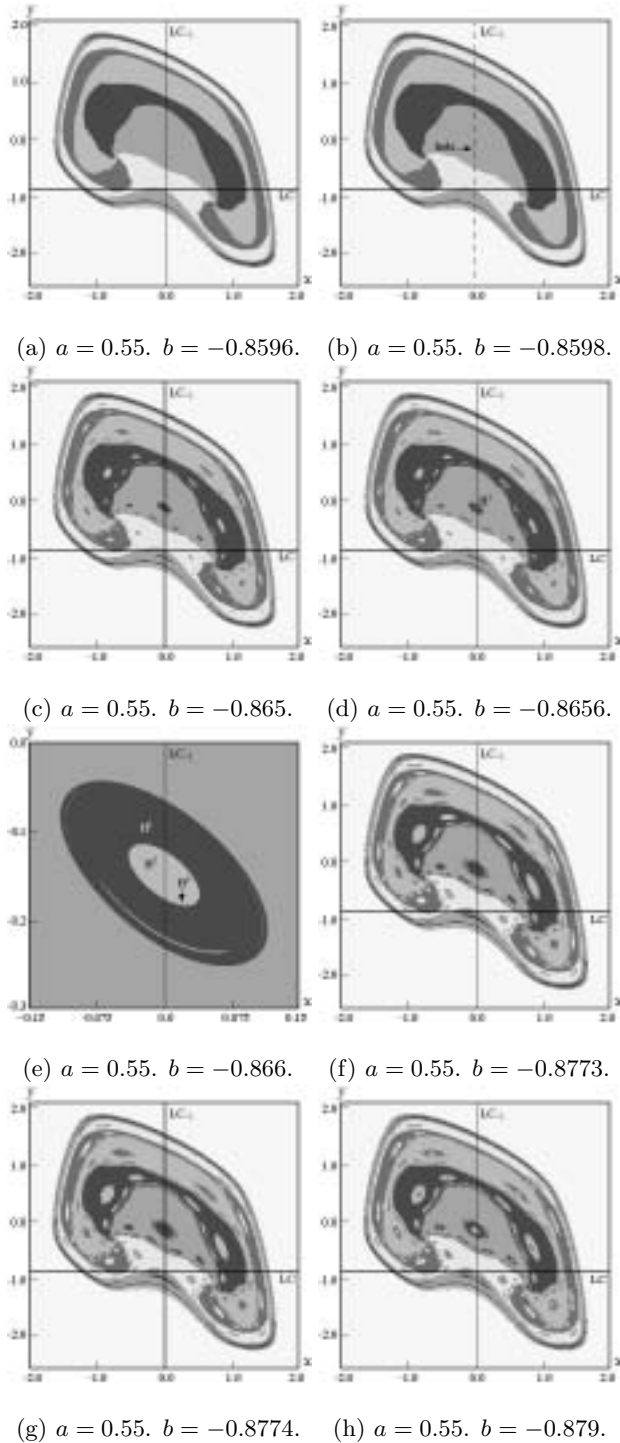


Figure 5: Basin of 5-periodic points for Eq. (12).

successive “simply connected basin  $\Leftrightarrow$  multiply connected basin” bifurcations which never reported, as far as we know. As a result of these bifurcations, there appear many holes in the basin and the basin structure becomes very complicated. Using our algorithm, we can clarify the parameter region in which the complicated basin bifurcations occur.

Our future problems are (1) to find a engineering application and (2) to applicate a higher-dimensional system.

### Acknowledgments

H. Kitajima would like to thank the members of *Groupe d’Etudes des Systèmes Non Linéaires et Applications* at the *Institut National des Sciences Appliquées de Toulouse*, for their encouragement during his stay. He also acknowledges Dr. Yoshinaga at the University of Tokushima for his helpful comments.

### References

- [1] C. Mira, *Systèmes Asservis Nonlinéaires*, ed. Hermès, Paris, 1990.
- [2] R.A. Adomaitis and I.G. Kevrekidis, “Noninvertibility and structure of basins of attraction in a model adaptive control system,” *J. Nonlinear Sci.* 1, pp.95–105, 1991.
- [3] L. Gardini, “On a model of financial crisis. Critical lines as new tools of global analysis,” in *Nonlinear Dynamics in Economics and Social Sciences*, ed. Gori & Geronazzo, Springer-Verlag, New York, 1993.
- [4] K. Aihara, “Chaotic neural networks,” in *Bifurcation Phenomena in Nonlinear Systems and Theory of Dynamical Systems*, ed. H. Kawakami, World Scientific, pp.143–161, 1989.
- [5] C. Mira, “Détermination pratique du domaine de stabilité d’un point d’équilibre d’une récurrence non-linéaire du deuxième order à variables réelles,” *Comptes Rendus Acad. Sc. Paris Série A* 261, groupe 2, pp. 5314–5317, 1964.
- [6] J.C. Cathala, “On some properties of absorptive areas in second order endomorphisms,” *Proc. ECIT Batschuns*, Austria, Sept. 89, World Scientific, Singapore, pp.42–54, 1991.
- [7] J.C. Cathala, “Basin properties in two-dimensional noninvertible maps,” *Int. J. Bifurcation and Chaos*, vol.8, no.11, pp.2147–2189, 1998.
- [8] C. Mira et al., “Basin bifurcations of two-dimensional noninvertible maps: fractalization of basins,” *Int. J. Bifurcation and Chaos*, vol.4, no.2, pp.343–381 1994.
- [9] G. Millerioux and C. Mira, “Homoclinic and heteroclinic situations specific to two-dimensional noninvertible maps,” *Int. J. Bifurcation and Chaos*, vol.7, no.1, pp.39–70 1997.
- [10] I. Gumowski and C. Mira, “Solutions chaotiques bornées d’une récurrence ou transformation ponctuelle du second ordre à inverse non-unique,” *Comptes Rendus Acad. Sc. Paris Série A* 285, pp.477-480 1977.
- [11] H. Kawakami and J. Matsuo, “Bifurcation of doubly asymptotic motions in nonlinear systems,” *IEICE Trans. Fundamentals*, vol.J65, no.7, pp.647–654, July 1982.
- [12] T. Yoshinaga, H. Kitajima, H. Kawakami and C. Mira, “A method to calculate homoclinic points of a two-dimensional noninvertible map,” *Trans. IEICE*, vol.E80-A, no.9, pp.1560–1566, Sep. 1997.
- [13] C.H. Nien and F.J. Wicklin “An algorithm for the computation of preimages in noninvertible mappings,” *Int. J. Bifurcation and Chaos*, vol.8, no.2, pp.415–422, 1998.
- [14] H. Kawakami, “Bifurcation of periodic responses in forced dynamic nonlinear circuits: computation of bifurcation values of the system parameters,” *IEEE Trans. Circuits & Syst.*, vol.CAS-31, no.3, pp.248–260, March 1984.